

Supporting Information

Kim et al. 10.1073/pnas.1714986115

SI Materials and Methods

Chemicals and Antibodies. Fura-2 AM and Lipofectamine 2000 were obtained from Invitrogen. TG and PMA were from Santa Cruz. 2-APB was from Sigma-Aldrich. Anti-Flag M2 affinity gel was obtained from Sigma. Antibodies targeting GFP (598; MBL International) and Flag (M2, F1804; Sigma) were purchased from the indicated vendor.

NFAT Nuclear-Translocation Assay. HEK293 cells were cultured on polyornithine-coated 15-mm round cover glasses. GFP-NFAT1 3 was transfected into cells with the indicated constructs. The culture medium was changed after 2 h, and cells were incubated for 18–24 h. The cells were washed three times with PBS and were fixed with 4% paraformaldehyde and mounted with Aqua-Poly/Mount solution (Polysciences) at room temperature. The cells were imaged using an IX83 microscope equipped with an Olympus 40× oil objective lens (NA 1.30), fluorescent lamp (Olympus), an LEP stage controller, and a CCD camera (Andor). Images were analyzed using Fiji software.

NFAT-Luciferase Assays. HEK293T cells were transfected with the NFAT reporter gene (15) and the indicated constructs. Cotransfection with the Renilla luciferase gene (*pRLTK*) was used as an internal control for cell number and transfection efficiency. After 12–18 h incubation, cells were treated with DMSO, 1 μ M PMA, or 1 μ M PMA + TG for 4–8 h. Assays were performed by the dual luciferase reporter assay system (Promega). For each condition, luciferase activity was measured in samples taken from duplicate wells with a 96-well automated luminometer (Bio-Rad). Results are calculated as the ratio of firefly to Renilla luciferase activity.

Immunoprecipitation and Immunoblot Analysis. HEK293T cells were transfected with the indicated constructs for 12–24 h. Transfected cells were washed three times with PBS and lysed by 50 mM Tris-HCl (pH 7.5), 150 mM NaCl, and 1% Triton X-100. Lysates were centrifuged at 9,700 \times *g* for 10 min, and the supernatant was incubated overnight at 4 °C with anti-Flag M2 agarose beads (Sigma). Lysates and immunoprecipitated samples were run on an SDS/PAGE system, probed with HRP-conjugated secondary antibody, and detected by enhanced chemiluminescence (Pierce).

Confocal Microscopy. Confocal fluorescence images were acquired on an LSM780 (NLO; Zeiss) confocal microscope with a Zeiss 100× oil objective lens (NA 1.46). mCherry and eGFP were excited simultaneously at 594 nm and 488 nm, respectively. Fluorescence emission was collected at 615–840 nm (mCherry) and 510–570 nm (eGFP). Zen software (Zeiss) was used for image acquisition. All experiments were performed at 25 °C.

TIRF Microscopy. TIRF fluorescence images were acquired with an Olympus IX81-ZDC inverted microscope with CellTIRF equipped with an Olympus UAPON 60× TIRF oil immersion objective (NA 1.49) and a CCD camera (Andor). Cells were excited at 488 or 594 nm, and fluorescence emission was collected at 485 nm (eGFP) and 575 nm (mCherry). xCellence software (Olympus) was used for image acquisition. All experiments were performed at 25 °C. Venus fluorescence was detected with a 100-mW, 488-nm laser with a 546-nm filter.

Intracellular Ca²⁺ Imaging. Cells were loaded with 1 μ M Fura-2 AM in DMEM at 37 °C for 30 min. Ratiometric Ca²⁺ imaging was performed at 340 and 380 nm in 0 or 2 mM Ca²⁺ Ringer's solution with a IDX81 microscope (Olympus) equipped with an

Olympus \times 40 oil objective lens (NA 1.30) and with a fluorescent arc lamp (LAMDA LS), excitation filter wheel (Lambda 10-2; Sutter Instruments), stage controller (MS-2000; ASI), and a CCD camera (C10600; Hamamatsu) at room temperature. Images were processed with MetaMorph software (Molecular Devices) and analyzed with Igor Pro software (WaveMetrics).

FRAP. Images were acquired on LSM780 confocal microscope with a Zeiss 63× oil lens (NA 1.46) at room temperature. Prebleached and recovery images were scanned at 488 nm at 2% power. A 0.4- μ m diameter circle was bleached with a full transmission for \sim 2 s. Bleaching during the recovery period was negligible (<4%). Images were analyzed with Zen software (Zeiss).

Electrophysiology. Patch-clamp experiments conditions were as previously described (15). Briefly, HEK293 cells were transfected 12–24 h before electrophysiology experiments with the indicated constructs by Lipofectamine 2000. Currents were recorded via standard whole-cell patch-clamp techniques (39). Pipettes with a resistance of 2–5 M Ω were filled with an internal solution containing 150 mM Cs-aspartate, 8 mM MgCl₂, 10 mM EGTA, and 10 mM Hepes (pH 7.2 with CsOH). Currents were sampled at 5 kHz and filtered at 2 kHz, and all voltages were corrected for the junction potential of the pipette solution relative to Ringer's solution in the bath (–13 mV). Data analysis was done with OriginPro software (OriginLab).

SPR-Binding Assays. SPR was performed with a BIAcore T200 instrument (GE Healthcare). All recombinant proteins were purified and analyzed with SDS/PAGE. The GST-23L of C.Orai1 was captured on CM5 S chip surfaces (GE Healthcare). 6 \times HIS tagged C.CAD was used as an analyte with variant concentrations. Binding assays were performed by injecting twofold serial dilutions of an analyte in HBS-EP buffer (GE Healthcare) at a flow rate of 30 μ L/min (for kinetic experiments). Surfaces were regenerated by a brief injection of 50 mM sodium hydroxide (60-s contact time at a flow rate of 60 μ L/min).

MD Simulations. The atomistic model for C.Orai1 was built based on homology modeling where the crystal structure of the *Drosophila melanogaster* Orai1(dOrai1) channel (PDB ID code 4HKR) was used as a template. Given the amino acid sequences of WT C.Orai1, a complete atomistic model was constructed using the I-TASSER (42) webserver from which the C.Orai1 protein's starting coordinates for MD were obtained.

C.Orai1 WT protein monomer was embedded in a phosphatidylcholine lipid bilayer and solvated with TIP3 model water and neutralized with sodium and chloride ions to yield a concentration of 150 mM NaCl. The simulation box size was 100 \times 75 \times 92 Å and contained \sim 74,000 atoms in total. This procedure of building an initial structure for MD was done with VMD software (University of Illinois at Urbana-Champaign), and protocols for minimization, annealing, equilibration, and successive MD runs were prepared by QwikMD (43). The resulting MD system was simulated by the NAMD MD package version 2.11 (44) in the constant pressure and temperature (NpT) condition. Pressure was maintained at 1 atm using the Langevin piston algorithm with an oscillation and damping timescale of 200 fs and 100 fs, respectively, and the temperature was kept at 300 K using Langevin dynamics. A distance cutoff of 12.0 Å was applied to short-range, nonbonded interactions, and a cutoff of 10.0 Å was used for the smothering functions. The particle-mesh Ewald (PME) method was used in treating long-range electrostatic

interactions. For integration equation of motion, the r-RESPA multiple time step scheme (44) was employed so that it could update the short-range interactions at every step and long-range electrostatics interactions at every two steps. The time step for integration was chosen to be 2 fs. SHAKE/RATTLE algorithms were utilized in constraining all bonds connected to hydrogens. The rmsd of protein was calculated to determine whether the MD system reached equilibrium. The RMSF of protein residues was obtained from the data points of MD simulation whose rmsd values were stable.

FRET Experiment. The FRET assay was performed by a previously reported method (45, 46). Fused proteins were expressed in HEK293 cells using Lipofectamine 2000 (Life Technologies). Images were acquired on an LSM780 microscope with a Zeiss 63× oil lens (NA 1.46) at room temperature. For mClover3, 488-nm laser excitation was used, with 500- to 600-nm light collected; for mRuby3, 559-nm laser excitation was used, with 570- to 670-nm light collected. For the FRET signal, 488-nm laser excitation was used, with 570- to 670-nm light collected. The FRET signal was calculated using MetaMorph software: FRET journal [FRET = $I_{\text{FRET}} - (B_{\text{Donor}} \times I_{\text{Donor}}) - (B_{\text{Acceptor}} \times I_{\text{Acceptor}})$], where B = bleed-through correction factors as determined by separate experiments using mClover3 only or mRuby3 only.

Plasmids. mCherry-H.STIM1 and EGFP-H.Orai1 plasmids were described previously (20). mCherry-H.CAD, GFP-NFAT, NFAT-firefly-Luciferase reporter, and pRLTK plasmids were described previously (15). C.STIM1 and C.Orai1 were amplified by PCR using the *C. elegans* CDNA library and the primer sets shown below. The PCR products were cloned into the pCR8-GW-TOPO cloning vector (Invitrogen). A KpnI site at the NT of C.STIM1 was generated to preserve signal sequence using the primer sets shown below and the QuikChange XL site-directed mutagenesis kit (Agilent Technologies). Entry clones of C.STIM1 and C.Orai1 constructs were transferred to the destination vectors by Gateway LR-Clonase reactions (Invitrogen) to generate the expression constructs. All plasmids were sequenced to verify the constructs.

Primers. The following primers were used.

For full-length C.Orai1 (amino acids 1–293).

Forward: 5-gccaccatgcctctgtcacacgatccatcccgc-3

Reverse: 5-tcagatatcccgaattgttgacggagcaag-3

For full-length C.STIM1 (amino acids 1–530).

Forward: 5-tctagagccaccatgggtagagtttctgtgattattgc-3

Reverse: 5-tccattagaagtgccaccagactg-3

For the C.STIM1 internal KpnI site.

Forward: 5-atacgggataaattgggtaccgaagcgattagatattc-3

Reverse: 5-gaatatctctaatgccttcggtaccatattatcccgtat-3

For the C.Orai1 NT (amino acids 1–121).

Forward: 5-ggatccgccaccatgcctctgtcacacgatccatcc-3

Reverse: 5-tcatctgaaactgcctttcagttgtgc-3

For the C.Orai1 23L (amino acids 170–199).

Forward: 5-ggatccgccaccactgtattctaccgtatatggaag-3

Reverse: 5-tcagagccatgacagatcaatgtagaa-3

For the C.Orai1 CT (amino acids 249–293).

Forward: 5-ggatccgccaccatttattgattcacaataatcgcgc-3

Reverse: 5-tcagatatcccgaattgttgacggagc-3

For C.CAD (amino acids 286–388).

Forward: 5-ggatccgccaccatggctctcttgcacttcagccattg-3

Reverse: 5-tcaatatagaagtggaaaaccgcaagtgttc-3

For C.Orai1-ΔNT.

Forward: 5-ggatccgccaccatgacgtcagcacttctggcagg-3

Reverse: 5-tccattagaagtgccaccagactg-3

For C.Orai1-ΔCT.

Forward: 5-tctagagccaccatgggtagagtttctgtgattattgc-3

Reverse: 5-agatctttaactgaacaccagcaatacaactc-3

For C.Orai1 ΔNT, ΔCT.

Forward: 5-ggatccgccaccatgacgtcagcacttctggcagg-3

Reverse: 5-agatctttaactgaacaccagcaatacaactc-3

For C.Orai1 (FY-RH), the C.Orai1 23L (FY-RH), and M3 peptide (FY-RH; F192R, Y193H). The C.Orai1 (FY-RH; F192R, Y193H) mutation was generated by substituting nucleotides at 574 (T → C), 575 (T → G), and 577 (T → C).

Forward: 5-cgcatattaagttgaagcggccaccattgatctgtcatggc-3

Reverse: 5-gccatgacagatcaatgtggcgttcaacttaatatgcg-3

For C.Orai1-ΔFY. The C.Orai1 (ΔFY; F192, Y193) mutation was generated by deleting nucleotides at 574 (T), 575 (T), 576 (C), 577 (T), 578 (A) and 579 (C).

Forward: 5-gattctccgatattaagttgaagattgatctgtcatggc-3

Reverse: 5-gccatgacagatcaatcttcaacttaatatgaggagaatc-3

For C.Orai1-ΔM3. C.Orai1-ΔM3 was constructed were by removing the nucleotides of the M3 domain and using the following primers:

Forward: 5-gtacacagttctccacgtcatcggtcttctg-3

Reverse: 5-ggtggagaactgtgtacatccagtagcttccatatacgg-3

For C.Orai1 (V271S) and C.Orai1 (V271D). The C.Orai1 (V271S) and (V271D) mutations were constructed by substituting nucleotides at 811 (G → T for V271S), 812 (T → C for V271S and T → A for V271D), and 813 (G → C for V271D).

For C.Orai1 (V271S).

Forward: 5-gattcaagcataagtcggacacaatgaagc-3

Reverse: 5-gcttcattgtgtccgacttatgcttgaatc-3

For C.Orai1 (V271D).

Forward: 5-gattcaagcataaggacgacacaatgaagc-3

Reverse: 5-gcttcattgtgtcgtcttctatgcttgaatc-3

For C.Orai1 (M274S) and C.Orai1 (M274D). The C.Orai1 (M274S) and (M274D) mutations were constructed by substituting nucleotides at 820 (A → T for M274S and G → G for M274D), 821 (T → C for M274S and T → A for M274D), and 822 (G → C for M274D).

For C.Orai1 (M274S).

Forward: 5-gcataaggtggacacagacaagcagttctctgacgt-3

Reverse: 5-acgtcaaggaactgctgtgtgttccaccttatgc-3

For C.Orai1 (M274D).

Forward: 5-gcataaggtggacacatcgaagcagttctctgacgt-3

Reverse: 5-acgtcaaggaactgctgtgtgttccaccttatgc-3

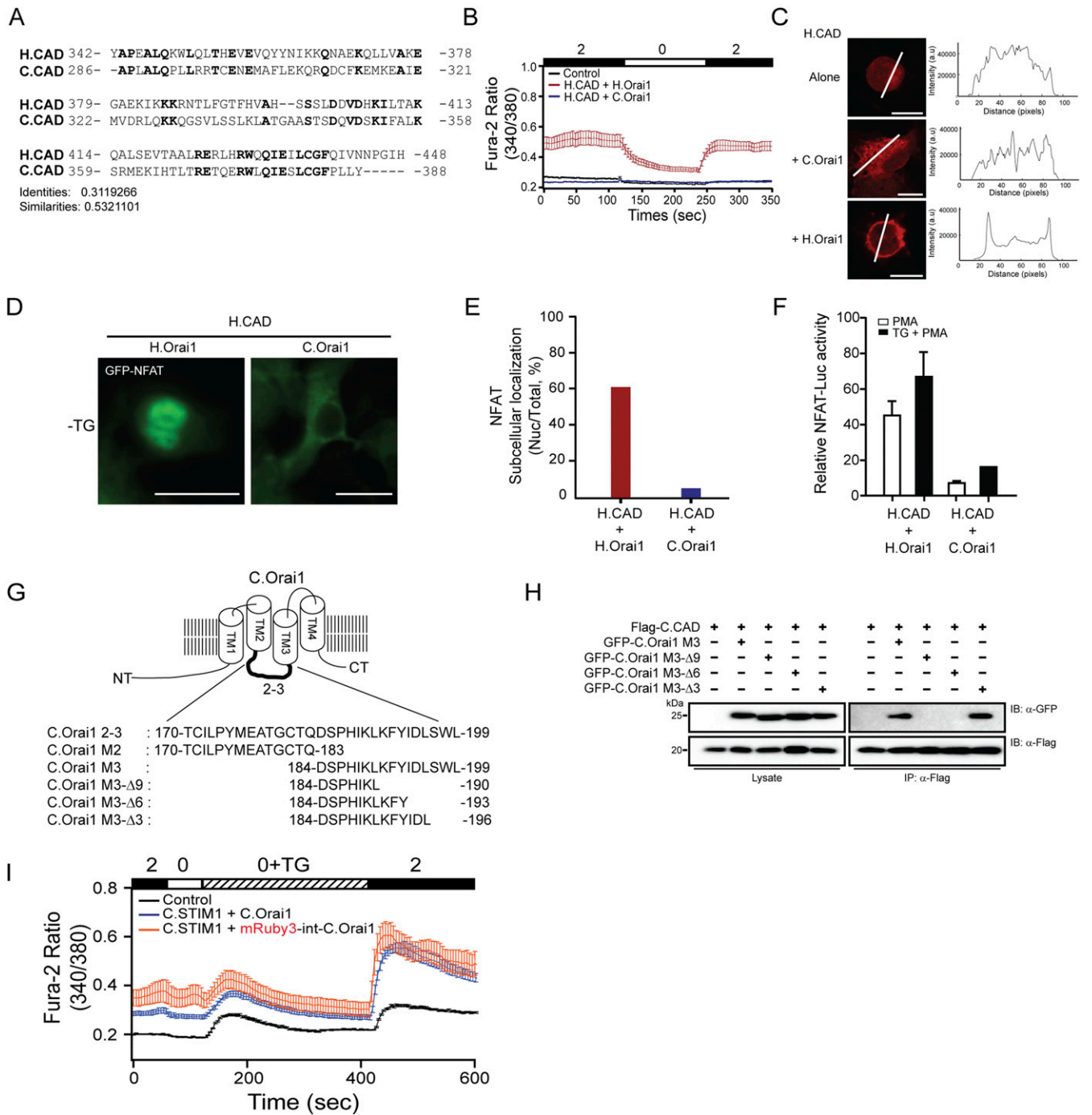


Fig. S2. The H.Orai1 CAD does not activate C.Orai1. (A) Sequence alignment of the CADs of H.Orai1 and C.Orai1, and conserved amino acids are shown in bold. (B) Human CAD with C.Orai1 did not activate SOCE. (C) Localization of Cherry-H.CAD alone (Top), with C.Orai1 (Middle), and with H.Orai1 (Bottom). Cherry-H.CAD did not accumulate at the PM when coexpressed with C.Orai1 (Middle). (D) Nuclear translocation of GFP-NFAT. (E) Histograms of the mean abundance of nuclear-translocated NFAT under the indicated conditions. (F) NFAT-dependent luciferase activity in cells expressing H.CAD and either C.Orai1 or H.Orai1. The cells were treated with PMA or with TG + PMA as indicated. The results are typical of at least three independent experiments. (G) Schematic representation of the 23L and truncated domains (M2, M3, M3-Δ9, M3-Δ6, and M3-Δ3) of C.Orai1. (H) FLAG-tagged C.CAD coimmunoprecipitated with the M3 and M3-Δ3 domains but not with M3-Δ6 and M3-Δ9 domains. (I) Fura-2 Ca^{2+} measurements in HEK293 cells expressing C.STIM1 with either C.Orai1 (blue) or mRuby3-int-C.Orai1 (orange). (All scale bars, 10 μm .)

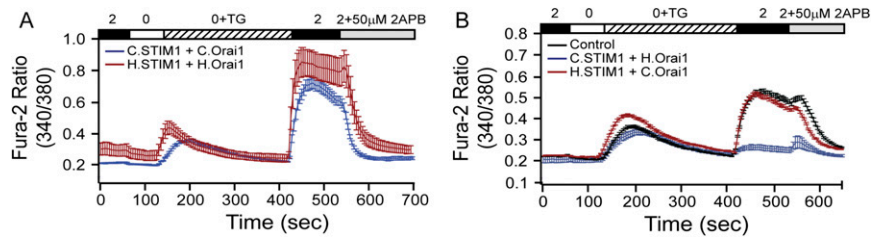


Fig. S3. The 2-APB treatment showed no potentiation of C.SOCE. (A and B) $[Ca^{2+}]_i$ measurements in cells expressing the indicated constructs with the treatment of 2-APB.

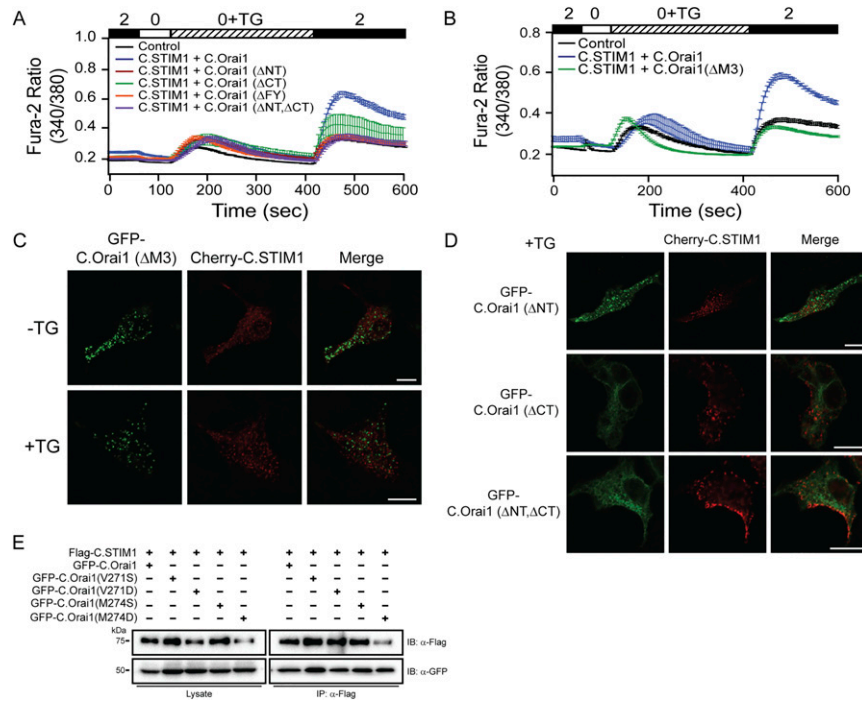


Fig. S4. The interaction between C.STIM1 and variant C.Orai1-mutant channels. (A) $[Ca^{2+}]_i$ measurements in cells expressing the indicated constructs. (B) Fura-2 Ca^{2+} measurements in HEK293 cells expressing C.STIM1 with either C.Orai1 (blue) or C.Orai1 ($\Delta M3$) (green). (C) Localization of Cherry-C.STIM1 with GFP-C.Orai1 ($\Delta M3$) with or without store depletion. (D) Localization of Cherry-C.STIM1 with GFP-C.Orai1 (ΔNT) (Top), with GFP-C.Orai1 (ΔCT) (Middle), and with GFP-C.Orai1 ($\Delta NT, \Delta CT$) (Bottom). (E) FLAG-tagged C.STIM1 coimmunoprecipitated with all GFP-tagged mutants C.Orai1.

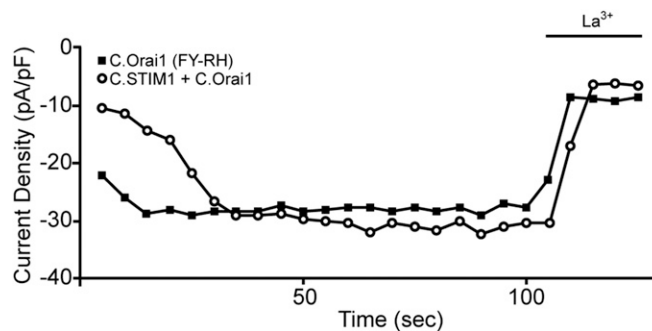


Fig. S5. Time-dependent induction of patch experiments. The I_{CRAC} time course of cells expressing C.Orai1 (FY-RH) alone or C.Orai1 with C.STIM1.